ZIBELINE INTERNATIONAL™ PUBLISHING

Engineering Heritage Journal (GWK)

DOI: http://doi.org/10.26480/gwk.01.2024.01.06

ISSN: 2521-0904 (Print)
ISSN: 2521-0440 (Online)
CODEN: EHJNA9

RESEARCH ARTICLE

APPLICABILITY OF 3D LASER SCANNING TECHNOLOGY IN MINING SUBSIDENCE MONITORING

Lihui Wang*, Rongfei Yang, Yong Lei, Chengcheng Fan, Jibo Liu, Chuanjian Ren

Guizhou University of Engineering Science, Bijie, 551700, China.
****Corresponding author email: 542246308@qq.com***

ARTICLE DETAILS

Article History:

Received 28 September 2023
Revised 01 November 2023
Accepted 04 December 2023
Available online 08 December 2023

ABSTRACT

3D laser scanning technology has been applied in mining subsidence monitoring to some extents. Based on the existing observation conditions in the experimental area, the laser point cloud data was collected; Then the methods of point cloud data denoising, registration, filtering and subsidence basin extraction were discussed. Finally, the processing results were analyzed and tested. The results show that: (1) The orientation method has better applicability in mining subsidence monitoring based on TLS, and can avoid the error accumulation caused by the registration method; (2) The error rate of the Irregular Triangulation filtering method with additional constraints on the selection of ground points is 4.22%, which is better than the fitting method; (3) The subsidence basin obtained by TLS has high accuracy, and the mean square error of the difference between TLS and surface subsidence measured by leveling is 3.3 cm.

KEYWORDS

3D laser scanning; Mining subsidence; Point cloud registration; Subsidence basin

1. INTRODUCTION

Conventional coal mine subsidence monitoring mainly uses GNSS, total stations, or leveling instruments to observe monitoring points, aiming to analyze the movement and deformation of the subsidence areas. The monitoring points are usually set up linearly along the strike and dip directions. Such methods have drawbacks including difficult monitoring point deployment, large workload, limited data acquisition, and inability to achieve full area coverage (Hu et al., 2013). Terrestrial laser scanning (TLS) offers the advantages of high speed, high accuracy, and large density, making it a strong complement to conventional monitoring methods. In the application of TLS technology, point cloud data processing is one of the key issues. Currently, many researchers have studied point cloud data processing techniques and have achieved significant results.

A studied accurate and fast denoising methods for laser scanning point clouds; Chen et al., 2014 analyzed and compared various methods for registering ground-based 3D laser point clouds; some researchers explored methods for target ball center positioning; researched improved methods based on TIN point cloud filtering (Li et al., 2015; Chen et al., 2014; Yu et al., 2019 and Lu et al., 2009; Zeng et al., 2016; Zhao et al., 2016). In disaster monitoring, deformation monitoring, building monitoring, and virtual reality, TLS technology has also achieved good application results (Yang et al., 2017). In the field of topographic surveying, some researchers have made beneficial attempts; some researchers discussed the techniques and processes of TLS applied in large-scale topographic mapping (Wang et al., 2018; Li et al., 2010). A limitation is that these experiments are often applied to small-area detailed topographic mapping, making it challenging to promote in broader topographic surveys (Wang, 2017).

The application of TLS technology in mining subsidence monitoring can be considered an extension of its use in topographic surveying. A group researchers discussed the data processing methods of TLS for mining subsidence monitoring and analyzed the sources of error; used TLS technology to monitor salt mine subsidence and compared it with wire measurements; in an effort to reduce errors from station point cloud stitching, combined GPS with TLS for subsidence monitoring (Hu et al., 2013; Tudor et al., 2016; Zhou et al., 2014). This paper studied the data processing methods of TLS technology in mining subsidence monitoring, and compared the subsidence measured by TLS with the leveling results, providing a reference for further research on the application of TLS technology in complex dynamic mining subsidence areas.

1.1 Survey Area and Data Collection

The mining subsidence area is generally large, exceeding the effective scanning distance of the scanner, so multiple station setups are required to cover the entire survey area. The rational layout of the stations should mainly consider the instrument range, topographical conditions, and the current state of subsidence in the survey area, in order to minimize environmental impacts and improve data collection quality and efficiency. The instrument used in the experiment is the RIEGL VZ4000, with a maximum scanning range of 4000m, a measuring speed of 147,000 points/s, a vertical scanning field of view from -30º to +30º, and an angular resolution better than 0.0005°. During the measurement, a connecting device was used to connect the GPS with the scanner. The height difference between the two instruments is about 20cm. A tilt of the scanner within 5° does not affect the accuracy of the GPS by more than 3mm and not more than 0.8mm in the vertical direction. The topography of the survey area is shown in Figure 1, with an area of about 1 Km2, characterized by slightly undulating plateau and hilly terrain, with a maximum height difference of 64m. The ground is mainly sparse grassland, bare ground, and a few scattered trees.

The survey stations are set up based on the terrain, ensuring good visibility and coverage of the entire survey area. Each station uses a 360° full-circle scanning method. At the same time, GNSS-RTK is connected to the scanner to collect the coordinates of each station, with the GNSS-RTK continuous collection time being approximately 10 minutes. The unification of the coordinate system of the survey area generally has two

Quick Response Code	Access this article online	
	Website: www.gwk.com.my	**DOI:** 10.26480/gwk.01.2024.01.06

Cite the Article: Lihui Wang, Rongfei Yang, Yong Lei, Chengcheng Fan, Jibo Liu, Chuanjian Ren (2024). Applicability of 3d Laser Scanning Technology in Mining Subsidence Monitoring. *Engineering Heritage Journal (GWK), 7(1): 01-06.*

methods: post-orientation using RTK or total station wire measurement combined with target balls, and parameter transformation based on the center coordinates of common target balls after registration (Yang et al., 2018). This paper uses the station coordinates measured by GNSS-RTK and orients with the target ball coordinates to achieve the unification of the coordinate systems of each survey station in the survey area.

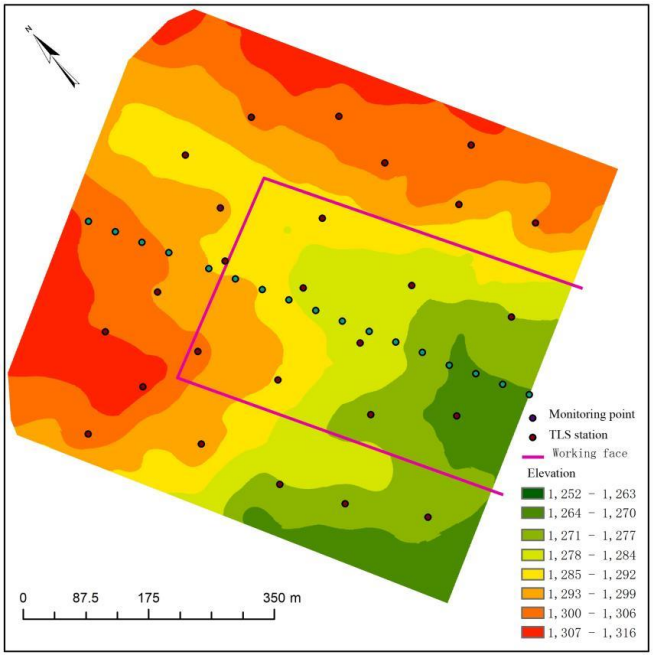

Figure 1: Overview of the Survey Area

2. Point Cloud Data Processing Method

2.1 Point Cloud Denoising

Noise points in the point cloud have a significant impact on subsequent operations. The noise in the laser point cloud includes low-bit gross errors and high-bit gross errors. The noise from ground-based laser radars is primarily high-bit gross errors, and the specific cause of the noise is generally unclear (Li et al., 2015). Point cloud denoising methods include statistical filtering, bilateral filtering, conditional filtering, and random sampling consensus filtering. Statistical filtering for point cloud denoising is a commonly used method. Its principle is to statistically analyze the neighborhood of each point and remove neighborhood points that do not meet the standard. The algorithm is to search for a specified number of neighboring points for each point, calculate the average distance from that point to the neighboring points, and then calculate the median and standard deviation of the distances. Points in the neighborhood set with distances greater than $\mu + std * \sigma$ (where μ is the median, *std* is the standard deviation, and σ is a multiple) are considered outliers and are removed. In this survey area, the number of neighborhood points is set to 10, and the standard deviation multiple is 5. These values can be adjusted based on the actual terrain.

2.1 Point Cloud Stitching

The three-dimensional orthogonal local coordinate system obtained by scanning with a ground-based 3D laser scanner is centered on the survey station. When the survey area is large, multiple station scans are required. Therefore, data from different stations need to be unified under the same coordinate system. This can be achieved using registration or orientation methods. Registering multi-station scan data hinges on finding common points between stations. Registration methods can be divided into feature-based registration and non-feature-based registration (Chen et al., 2014). Feature-based registration involves finding common feature points between stations and solving registration parameters using these common feature points (Liang et al., 2018). The orientation method involves inputting station coordinates measured by GNSS-RTK during station setup and orienting with target ball coordinates to unify the coordinate system of station data (Hu et al., 2013). This paper uses the orientation method, which avoids the error accumulation of station-by-station registration.

The key to the orientation method is to obtain the center coordinates of the target ball. The process is to first eliminate the anomalies of the target ball, then extract the center coordinates of the target ball through the algorithm, and then orient by minimizing the standard deviation between the center coordinates of multiple target balls and the coordinates measured by RTK. The single measurement accuracy of the scanner is 10mm, and the accuracy of the geometric model obtained by the least squares method can reach about 1mm (Zhang et al., 2008). The point cloud of the target ball obtained by scanning is a hemispherical surface. After selecting the point cloud of the target ball, the anomalies are manually removed, and then the center coordinates are extracted through the algorithm. For this, let the center coordinates and radius of the target ball be (x_0, y_0, z_0) and r, and the spherical point cloud be (x_i, y_i, z_i) (i=1,2,3....n), then the spherical equation is :

$$r = \sqrt{(x_i - x_0)^2 + (y_i - y_0)^2 + (z_i - z_0)^2} \quad (1)$$

Expanding and setting $x_0^2 + y_0^2 + z_0^2 - r^2 = d$, then equation (1) can be simplified as:

$$x_i^2 + y_i^2 + z_i^2 - ax_i - by_i - cz_i + d = 0 \quad (2)$$

Where a, b, c, and d are the parameters to be sought.

According to the least squares method, the value of $v = \sum_{i=1}^{n}(x_i^2 + y_i^2 + z_i^2 - ax_i - by_i - cz_i + d)^2$ should be minimized.

Using matrix method, we get:

$$\begin{bmatrix} a \\ b \\ c \\ d \end{bmatrix} = \begin{bmatrix} \sum x_i^2 & \sum x_i y_i & \sum x_i z_i & -\sum x_i \\ \sum x_i y_i & \sum y_i^2 & \sum y_i z_i & -\sum y_i \\ \sum x_i z_i & \sum y_i z_i & \sum z_i^2 & -\sum z_i \\ -\sum x_i & -\sum y_i & -\sum z_i & n \end{bmatrix}^{-1} \begin{bmatrix} \sum x_i(x_i^2 + y_i^2 + y_i^2) \\ \sum y_i(x_i^2 + y_i^2 + y_i^2) \\ \sum z_i(x_i^2 + y_i^2 + y_i^2) \\ -\sum(x_i^2 + y_i^2 + y_i^2) \end{bmatrix} \quad (3)$$

Based on the formula (3), parameters a, b, c, and d were calculated, leading to the determination of the center coordinates of the target ball, as seen in formula (4).

$$x_0 = \frac{a}{2}, y_0 = \frac{b}{2}, z_0 = \frac{c}{2}, r = \sqrt{x_0^2 + y_0^2 + z_0^2 - d} \quad (4)$$

To verify the precision of the aforementioned method, a random hemispherical data was generated using Matlab with Gaussian noise added. The center coordinates of the noisy hemispherical data were then determined and compared with the design value, as shown in Figure 2. The actual coordinates and radius of the test hemisphere were set to (100,10,80) and 3, respectively. According to the fitting results of the aforementioned method, the values were (100.0214,10.0258,80.0488) and 2.9979. Compared to the design values, the planar position differed by 0.03, and the relative error of the radius was 0.07%. Converted to a target ball with a radius of 7.5 cm, the error is 0.05 mm.

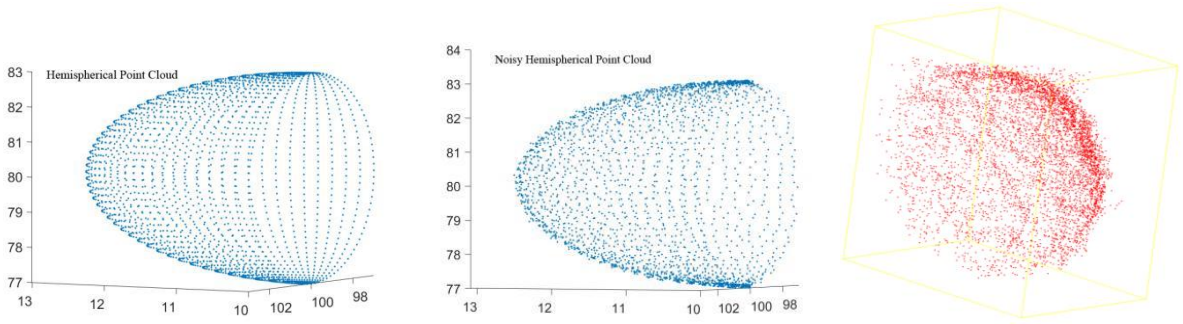

a. Hemispherical Point Cloud b. Noisy Hemispherical Point Cloud c. Actual Target Ball Point Cloud

Figure 2: Simulated Hemispherical Point Cloud vs. Actual Target Ball Point Cloud

The orientation method doesn't involve point cloud registration. It uses the station coordinates measured by GNSS-RTK as the center coordinates of the station, and orients using the RTK coordinates measured around the station's target ball piles. To maximize the orientation accuracy, orientation is carried out for multiple target ball piles based on the minimum mean error. The advantage of the orientation method is that the stations are independent of each other, reducing the cumulative error brought by registration.

2.3 Point Cloud Filtering

Many scholars have conducted research on point cloud filtering. Among them, the filtering method based on the Triangulated Irregular Network (TIN) has a good effect (Zhao X et al., 2016). This algorithm was first proposed by Axelsson. It generates a sparse triangular network through ground seed points and then iteratively refines the network layer by layer until all ground points are extracted (Zeng et al., 2016). To reduce the occurrence of non-ground points being misclassified as ground points, this paper added constraints to the selection of ground points based on the work of Zhao X and Ding Shaopeng. The specific process is as follows:

2.3.1 Selection of Ground Seed Points

After registration, a regular grid index is established for the point cloud. The grid size is slightly larger than the maximum building size in the survey area to avoid selecting points on buildings as seed points. The survey area in this case is a sparsely vegetated arid zone. A few scattered buildings have been demolished, and it's a plateau hilly area with gentle undulations. To accommodate steep slopes and the size of the tree canopy in the survey area, a grid size of 5m was chosen.

After the statistical grid is set up, the number of points in each grid is counted. Since ground points are continuous and the point cloud density is denser the closer it is to the station, if the number of points is less than a threshold n (determined based on grid size and actual conditions), the grid is considered noise and set to empty. The lowest point in each grid is chosen as the ground seed point. If all points in the grid are above the ground and non-ground points, as shown in Figure 3, then the selected ground seed point will also be a non-ground point. At this time, height difference is used for judgment. The height difference threshold H is set to twice the grid length (adjusted according to the grid size). The height difference $\Delta H_i (i = 1,2 \cdots 8)$between the center point and the seed points in the 8 neighboring grids is calculated. If the number of ΔH values greater than H is 8, then the point is considered a non-ground point and removed.

2.3.2 Construct the Triangular Network And Iterate To Densify

Use the selected seed points to build the initial triangular network, and then densify the irregular triangular network. The specific process is to traverse all points, calculate the distance d of the point to its triangle, and the maximum angle formed by the point to the 3 vertices and the plane where the triangle lies, as shown in Figure 4. Compare them with the iterative distance and iterative angle respectively. If they are less than the corresponding thresholds, the point is determined to be a ground point. Repeat this process until all ground points are extracted.

The expression for the plane where the triangle lies is as follows:

$$Ax + By + Cz + D = 0 \tag{5}$$

Thus, the distance d from the spatial point P(x0, y0, z0) to the plane where the triangle lies, and the angle a_i formed by the point with the 3 vertices and the plane where the triangle is located are given by equations (6) and (7), respectively.

$$d = \frac{|Ax+By+Cz+D|}{\sqrt{A^2+B^2+C^2}} \tag{6}$$

$$a_i = arcsin\frac{d}{s_{ip}} \tag{7}$$

Where i=1,2,3 ； Sip is the length from P to the corresponding vertex.

The TIN iterative densification algorithm uses the angle α_i threshold and the distance d threshold as filtering parameters to continuously densify the triangular network to extract ground points. Factors influencing the speed of TIN filtering mainly lie in the time consumed in densifying TIN (Kang et al., 2013). After the first filtering, trees, shrubs, and airborne cluster points are filtered out; during the second filtering, the grid size is reduced to half of the original. After two iterative filtering steps, the result of the third filtering hasn't changed much and ground points are well obtained, so the filtering can be stopped.

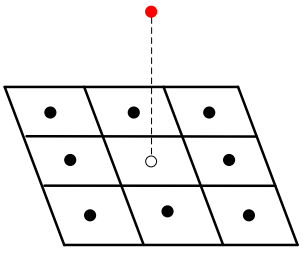

Figure 3: Center point too high relative to 8 neighboring points

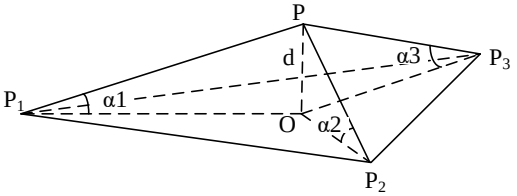

Figure 4: Schematic of the improved TIN densification principle

3. Results and Analysis

3.1 Orientation Analysis

Both coordinate transformations after registration and orientation can achieve the conversion of station coordinates to the local coordinate system. Errors originate from the accuracy of the scanner itself, RTK measurement errors, registration errors, and orientation errors, etc. The accuracy of the scanner measurement depends on the instrument itself. Besides the observation duration and distance from the base station, the main source of RTK measurement error comes from the multipath effect, which is greatly related to the environment (Kalyanaraman et al., 2019). Figure 5 shows the measurement results of an RTK from a certain station in the survey area for nearly 90 minutes. From the figure, it can be seen that the elevation measurement values change irregularly. It is generally believed that the error of the multipath effect is about several centimeters (Mekik et al., 2010). Therefore, long-duration observations are used to take the average to improve coordinate accuracy. Using the moving average method, the coordinate data of Figure 5 is averaged every 600 epochs (10 minutes). The calculated mean square error compared to the mean elevation measured over 90 minutes is 8mm, and the planar position mean square error is 2.3mm.

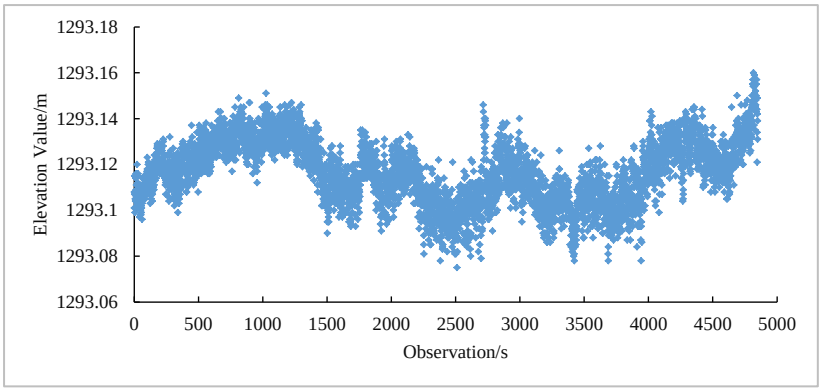

Figure 5: Multipath effect of RTK measurements from a certain station in the survey area

Each station's GNSS-RTK observation duration is 10 minutes. As can also be seen from Figure 5, the observation of dozens of epochs for the target ball RTK hardly improves accuracy. Therefore, during orientation, multiple targets are oriented based on minimizing the mean square error to enhance the orientation accuracy.

3.2 Point Cloud Filtering Analysis

Figure 6 shows an area of approximately 50m x 50m near a dirt pit, including the basin of the dirt pit, steeper slopes, and relatively flat ground. Nearby there are trees and wild grasses, representing the main terrain of the research area. The pit is relatively flat and has no vegetation cover, and the slope of the side slope is about 0.8. Figure 6(b) shows the post-filtering effect. Compared to the original point cloud, the trees have been filtered out, and the ground is largely retained, with no obvious noise remnants. The analysis results indicate that the algorithm in this paper can filter out the vast majority of the features in the point cloud, and both slopes and ground can be well retained.

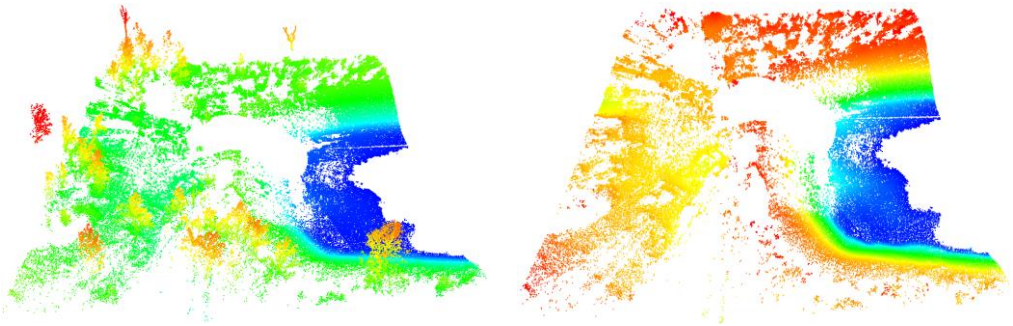

(a) Original Point Cloud (b) Filtering Effect

Figure 6: Comparison of Point Cloud Filtering Effects for the Dirt Pit

During the process of constructing TIN and selecting ground points, if the angle α and distance d thresholds are too large, some non-ground points close to the ground cannot be filtered out. If the threshold is too small, over-filtering may occur, resulting in the loss of some ground points. In this experiment, the maximum angle α and distance d thresholds are set to 8° and 0.5m, respectively. To further verify the filtering effect, this paper's method is compared with the fitting method. The fitting method locally fits the surface from the lowest point, calculates the distance from the point to the surface, and sets a threshold of 0.5m for filtering. Manually divide the point cloud in this data into ground points (GP) and non-ground points (NGP). The ground points filtered out by the filtering method are denoted as FGP, and the points wrongly classified as ground points are represented by EGP. The misclassification rate δ represents the ground point filtering accuracy:

$$\delta = \frac{|FGP+EGP|}{GP+NGP} \times 100\% \quad (8)$$

Table 1: Filtering Accuracy Analysis

Filtering Method	GP	NGP	FGP	EGP	δ
Method proposed in this paper	2260482	1512846	139126	20478	4.22
Fitting Method	2260482	1512846	197092	41086	6.31

From Table 1, it can be seen that for the sample data, the misclassification rate of the filtering method in this paper is 4.22%, which is better than the fitting method, and can be well applied to the point cloud filtering of this research area.

3.3 Accuracy Analysis of Subsidence Basin

The change in the DEM of the same area before and after coal mining is the subsidence basin of that area. The three-dimensional laser point cloud has a high density, which allows for the construction of a detailed DEM to extract the subsidence basin. The terrain surface modeling method based on triangles can well maintain the accuracy of the original data and can adapt to complex terrain changes. Based on the point cloud data from two periods, two grid DEMs can be obtained and differentiated to obtain the subsidence basin of the survey area, as shown in Figure 7.

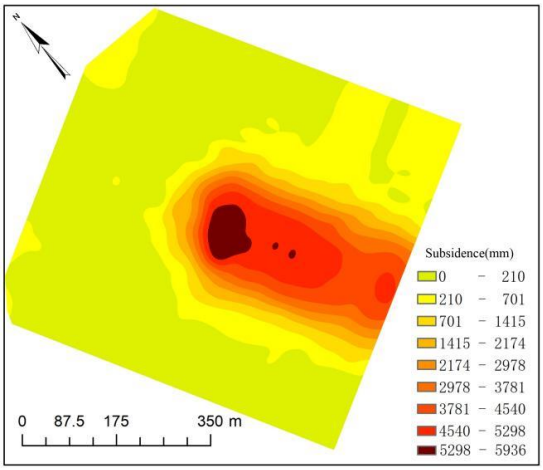

Figure 7: Subsidence Basin Map

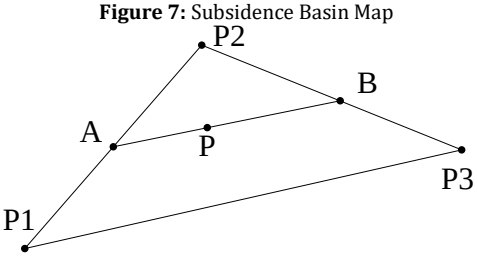

Figure 8: Bilinear Interpolation

In the TIN surface model, the elevation of trend and inclination monitoring points is obtained using interpolation methods for comparison with the leveling measurement results. This paper uses the bilinear interpolation method to obtain the elevation at a certain position in the TIN, as shown in Figure 8.

In the TIN, the three vertices of the triangle (P1, P2, P3) are known points, and P is any elevation undetermined point inside it. The idea of the bilinear interpolation method is to first draw a straight line through the point P intersecting the TIN at points A and B. Linear interpolations are performed on the edges P1P2 and P2P3 to obtain the elevations of points A and B. Then, a linear interpolation is performed on AB to get the elevation of point P. Figure 9 compares the subsidence values of 17 monitoring points on the trend line measured by leveling with those measured by the TLS method. The subsidence curves obtained by the two methods are basically consistent. The mean error of the subsidence difference measured by TLS and leveling is 3.3 cm, indicating high accuracy. This shows that TLS is a reliable method to capture the entire subsidence basin.

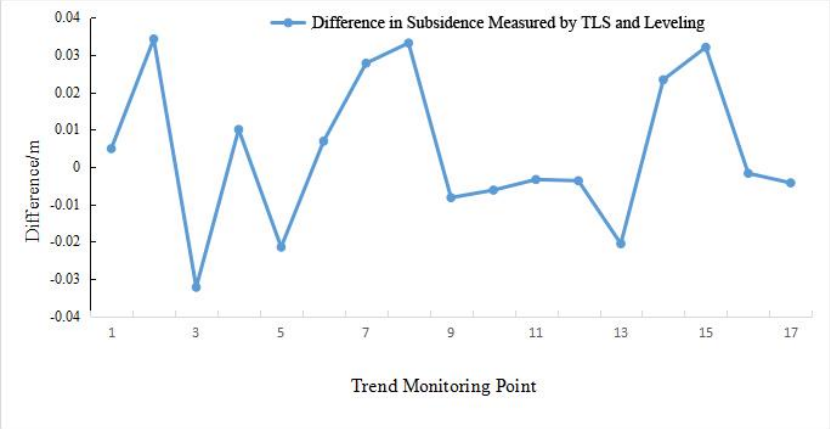

Figure 9: Difference in Subsidence Measured by TLS and Leveling

4. Conclusion

This paper discusses point cloud data denoising, registration, filtering, and coal mining subsidence basin extraction methods, and finally analyzes the accuracy of the results. The following conclusions are drawn:

(1) The orientation method is more applicable in TLS subsidence monitoring in mining areas, and its positioning accuracy depends on RTK accuracy. Orienting based on multiple target balls with the smallest mean error can improve orientation accuracy, avoiding the error accumulation brought about by the registration method.

(2) The irregular triangular network filtering method with added ground point selection constraints has a misclassification rate of 4.22%, which is superior to the fitting method.

(3) The subsidence basin obtained by TLS has high accuracy. The mean error of the difference in subsidence measured by TLS and leveling is 3.3 cm, indicating that TLS is a reliable method for capturing the entire subsidence basin.

Fund Program

Guizhou Provincial Department of Education Youth Science and Technology Talent Growth Project (Qian Jiao He KY Zi [2020]156, Qian Jiao He KY Zi [2020]149, Qian Jiao He KY Zi [2022]132); Guizhou High-level Innovative Talent Project (Bi Ke Talent He Zi [2021]09, Bi Ke Union Zi G [2019]15).

References

Bisheng, Y., Fuxun, L., Ronggang, H., 2017. Research Progress, Challenges, and Trends in 3D Laser Scanning Point Cloud Data Processing. Journal of Surveying and Mapping, 46 (10), Pp. 1509-1516.

Dahe, H., Kan, W., Ranli, C., 2018. Study on 3D Laser Scanning for Mining Subsidence Monitoring. Coal Mining, 18 (01), Pp. 20-22+35.

Feng, W., 2017. Method of Measuring Topography with 3D Laser Scanning Technology Integrated with RTK. Surveying and Mapping Bulletin, (03), Pp. 71-75.

Kalyanaraman, S., Braasch, M., Kelly, J., 2019. Influence of GPS Code Tracking on Carrier-Phase Multipath Performance.

Liang, C., Song, C., Xiaoqiang, L., 2018. Registration of Laser Scanning Point Clouds: A Review. Sensors, 18 (5), Pp. 1641.

Liang, L., Kan, W., Hu, L., 2010. Algorithm and Implementation of Gross Error Elimination for Ground 3D Laser Scanning Topographic Measurement Data. Science of Surveying and Mapping, 35 (03), Pp. 187-189.

Liangliang, C., Lichun, S., Tao, J., 2014. Ground 3D Laser Scanning Data Registration Method. Surveying and Mapping Bulletin, (05), Pp. 80-82.

Mekik, Ç., and Can, O., 2010. Multipath effects in RTK GPS and a case study. Journal of Aeronautics, Astronautics and Aviation, Series A., 42, Pp. 231-240.

Min, Y., Shu, G., Xiping, Y., 2018. Experiment on Ground 3D Laser Scanning Point Cloud Data Acquisition and Registration Processing under Complex Striped Terrain Conditions. Surveying and Mapping Bulletin, 494 (05), Pp. 38-43.

Minglei, L., Guangyun, L., Wenpeng, Z., 2015. Accurate and Rapid Noise Reduction Method for Laser Scanning Point Cloud. Surveying and Mapping Bulletin, (12), Pp. 27-29.

Nihong, Z., Yingchun, Y., Zhanying, W., 2016. Improved Irregular Triangular Network Dense Method for Vehicle-borne LiDAR Point Cloud Filtering. Science of Surveying and Mapping, 41 (09), Pp. 136-139+46.

Renyin, W., Kaiwei, L., Rui, C., 2018. Application of 3D Laser Scanning Technology in Topographic Mapping. Surveying and Mapping Bulletin, (12), Pp. 159-162.

Shu, Z., Kan, W., Xianglei, W., 2008. Discussion on the Application Issues of 3D Laser Scanning Technology in Subsidence Monitoring. Coal Science and Technology, (11), Pp. 96-99.

Teng, Y., Mingfeng, L., Wusheng, H., 2019. Research on Center Fitting of Spherical Target Based on Point Cloud Denoising. Geodetic Surveying and Earth Dynamics, 39 (08), Pp. 849-855.

Tieding, L., Shijian, Z., Liting, Z., 2009. Ground Laser Scanning Target Ball Positioning Method Based on Whole Least Squares. Geodetic Surveying and Earth Dynamics, 29 (04), Pp. 102-105.

Tudor, S., Rusu, T., Onose, D., 2016. The Use of Laser Scanning Technology In Land Monitoring Of Mining Areas. Carpathian Journal of Earth & Environmental Sciences, 11 (2), Pp. 565-573.

Xiaochen, K., Jiping, L., Xiangguo, L., 2013. Progressive Triangular Network Dense Filtering Method for Airborne LiDAR Point Cloud on Multicore Processors. Journal of Surveying and Mapping, 42 (3), Pp. 331-336.

Zhao, X., Guo, Q., Su, Y., 2016. Improved progressive TIN densification filtering algorithm for airborne LiDAR data in forested areas. ISPRS Journal of Photogrammetry and Remote Sensing, 117, Pp. 79-91.

Zhou, D., Wu, K., Chen, R., 2014. GPS/terrestrial 3D laser scanner combined monitoring technology for coal mining subsidence: a case study of a coal mining area in Hebei, China. Natural Hazards, 70 (2), Pp. 1197-1208.